

# Gaia16apd – a link between fast-and slowly-declining type I superluminous supernovae

T. Kangas<sup>1\*</sup>, N. Blagorodnova<sup>2</sup>, S. Mattila<sup>1</sup>, P. Lundqvist<sup>3</sup>, M. Fraser<sup>4,5</sup>,  
L. K. Hardy<sup>6</sup>, M. D. Stritzinger<sup>7</sup>, E. Cappellaro<sup>8</sup>, N. Elias-Rosa<sup>8</sup>, J. Harmanen<sup>1</sup>,  
E. Y. Hsiao<sup>9</sup>, E. Kankare<sup>10</sup>, M. B. Nielsen<sup>7</sup>, T. M. Reynolds<sup>1,11</sup>, L. Rhodes<sup>6</sup>,  
A. Somero<sup>1</sup> and Ł. Wyrzykowski<sup>12</sup>

<sup>1</sup>*Tuorla Observatory, Department of Physics and Astronomy, University of Turku, Väisäläntie 20, FI-21500 Piikkiö, Finland*

<sup>2</sup>*Cahill Center for Astrophysics, California Institute of Technology, Pasadena, CA 91125, USA*

<sup>3</sup>*Department of Astronomy and The Oskar Klein Centre, AlbaNova University Center, Stockholm University, SE-10691 Sweden*

<sup>4</sup>*Institute of Astronomy, University of Cambridge, Madingley Road, Cambridge CB3 0HA, United Kingdom*

<sup>5</sup>*School of Physics, O'Brien Centre for Science North, University College Dublin, Belfield, Dublin 4, Ireland*

<sup>6</sup>*Department of Physics and Astronomy, University of Sheffield, Sheffield, S3 7RH, UK*

<sup>7</sup>*Department of Physics and Astronomy, Aarhus University, Ny Munkegade 120, DK-8000 Aarhus C, Denmark*

<sup>8</sup>*INAF - Osservatorio Astronomico di Padova, Vicolo dell'Osservatorio 5, Padova I-35122, Italy*

<sup>9</sup>*Department of Physics, Florida State University, 77 Chieftain Way, Tallahassee, FL 32306, USA*

<sup>10</sup>*Astrophysics Research Centre, School of Mathematics and Physics, Queen's University Belfast, Belfast BT7 1NN, UK*

<sup>11</sup>*Nordic Optical Telescope, Apartado 474, E-38700 Santa Cruz de La Palma, Spain*

<sup>12</sup>*Warsaw University Astronomical Observatory, Al. Ujazdowskie 4, 00-478 Warszawa, Poland*

Accepted XXX. Received YYY; in original form ZZZ

## ABSTRACT

We present ultraviolet, optical and infrared photometry and optical spectroscopy of the type Ic superluminous supernova (SLSN) Gaia16apd, covering its evolution from 27 d before the *g*-band peak to the nebular phase, including the latest spectrum ever obtained for a fast-declining type Ic SLSN at 150.9 d. Gaia16apd is one of the closest SLSNe known ( $z = 0.102 \pm 0.001$ ), with detailed optical and *Swift* ultraviolet (UV) band observations covering the peak. Gaia16apd is a spectroscopically typical type Ic SLSN, exhibiting the characteristic blue early spectra with O II absorption, and reaches a peak  $M_g = -21.8 \pm 0.1$  mag. However, photometrically it exhibits an evolution intermediate between the fast- and slowly-declining type Ic SLSNe, with an early evolution closer to the fast-declining events. It is unusually UV-bright even for a SLSN, reaching a non-*K*-corrected  $M_{uvrm2} \simeq -23.2$  mag, the only other type Ic SLSN with similar UV brightness being SN 2010gx. This event highlights the importance of good rest-frame UV coverage for understanding SLSNe. Assuming that the event was powered by magnetar spin-down, we derive a period of  $P = 1.9^{+0.3}_{-0.2}$  ms and a magnetic field of  $B = 2.1^{+0.5}_{-0.2} \times 10^{14}$  G for the magnetar. The estimated ejecta mass is between 6 and 13  $M_\odot$  and the kinetic energy between  $1.0$  and  $2.1 \times 10^{52}$  erg, depending on opacity. The 150.9 d spectrum shows a remarkable similarity to slowly-declining type Ic SLSNe at late times and implies that the two classes originate from similar progenitors.

**Key words:** supernovae: individual (Gaia16apd) – stars: massive – stars: magnetars

## 1 INTRODUCTION

Superluminous supernovae (SLSNe) are explosions of massive stars that reach peak absolute magnitudes  $\leq -21$  mag

(e.g. Quimby et al. 2011; Gal-Yam 2012), making them up to hundreds of times brighter than normal supernovae (SNe). Like normal core-collapse supernovae (CCSNe), SLSNe are divided into hydrogen-rich (type II) and hydrogen-poor (type I) events based on their spectroscopy. Some SLSNe evolve to spectroscopically resemble normal type Ic SNe a

\* E-mail: tjakan@utu.fi

few weeks after maximum light (e.g. Pastorello et al. 2010; Inserra et al. 2013) and are called type Ic SLSNe. They are rare events, with an estimated rate of 0.01 per cent of the CCSN rates (Quimby et al. 2013; McCrum et al. 2015). The host galaxies of type Ic SLSNe are typically faint and metal-poor (e.g. Chen et al. 2013, 2015; Perley et al. 2016), and low metallicity has been suggested to be necessary for their progenitors. Type Ic SLSNe include both slowly declining events such as SN 2007bi (Gal-Yam et al. 2009), PTF12dam (Nicholl et al. 2013) or SN 2015bn (Nicholl et al. 2016b), and significantly faster-declining events such as SN 2010gx (Pastorello et al. 2010) or SN 2011ke (Inserra et al. 2013). The  $e$ -folding decline time-scales of fast- and slowly-declining events are clustered around 30 d and 70 d respectively, but this bimodality may not be significant (Nicholl et al. 2015).

Different power sources have been suggested to account for the high luminosity of SLSNe. Slowly declining SN 2007bi-like events (e.g. Gal-Yam et al. 2009) have been suggested to be pair-instability SNe (PISNe; Heger & Woosley 2002), where an extremely massive star is completely disrupted in a thermonuclear runaway process. However, in recent studies (e.g. Dessart et al. 2013; Nicholl et al. 2013; McCrum et al. 2014; Lunnan et al. 2016) such events have been found incompatible with PISN models (Kasen et al. 2011). The decay of  $^{56}\text{Ni}$  cannot be the primary power source, as it fails to produce both the required peak luminosity and the tail-phase light curve self-consistently (Quimby et al. 2011). Interaction with a circumstellar medium (CSM) remains a plausible way to power at least some SLSNe (e.g. Chevalier & Irwin 2011); however, fine-tuning of the CSM mass and density is required in order to explain some of the observational properties of type Ic SLSNe (Nicholl et al. 2015). Furthermore, type Ic SLSNe do not show signs of CSM interaction in their spectra (e.g. Nicholl et al. 2014). The currently dominant explanation for the luminosity is a central engine such as the spin-down of a millisecond magnetar with  $B \sim 10^{14}$  G (Kasen & Bildsten 2010; Woosley 2010) or possibly accretion onto a black hole from fall-back of ejected material (Dexter & Kasen 2013).

In this paper, we present photometric and spectroscopic observations and analysis of the type Ic SLSN Gaia16apd. We show that, early on, this event resembles the ‘prototypical’ fast-declining type Ic SLSN, SN 2010gx, but is located much closer and has been observed with better wavelength coverage. Later it evolves in a way intermediate between the fast- and slowly-declining type Ic SLSNe. Gaia16apd exhibits an ultraviolet (UV) brightness much higher than slowly-declining type Ic SLSNe, and is one of a scant few fast-declining type Ic SLSNe so far with good UV sampling, highlighting the necessity of UV observations for understanding the variation inside this class of SLSNe. We use magnetar light curve models to estimate physical parameters for the explosion and compare a late-time (150.9 d after maximum light) spectrum to the slowly-declining events.

## 2 OBSERVATIONS AND DATA REDUCTION

Throughout the paper, we assume a flat  $\Lambda$ CDM cosmology with  $H_0 = 69.6 \text{ km s}^{-1} \text{ Mpc}^{-1}$ ,  $\Omega_M = 0.286$  and  $\Omega_\Lambda = 0.714$  (Bennett et al. 2014). The redshift of the SN ( $z = 0.102 \pm 0.001$ ; see Section 2.2) corresponds to a luminosity

distance  $d_L = 473.3^{+5.0}_{-4.9} \text{ Mpc}$  and a distance modulus of  $\mu = 38.38 \pm 0.03$ . A Galactic reddening of  $E(B - V)_{\text{gal}} = 0.0132$  mag was adopted using the Galactic dust maps by Schlafly & Finkbeiner (2011).

### 2.1 Discovery and classification

Gaia16apd was discovered by the *Gaia* Photometric Science Alerts programme<sup>1</sup> of the *Gaia* satellite (Gaia Collaboration 2016) operated by the European Space Agency (ESA) on 2016 May 16.80 UT (MJD = 57524.80) at  $\alpha = 12^{\text{h}}02^{\text{m}}51^{\text{s}}.71$ ,  $\delta = +44^\circ15'27''.40$  (J2000.0) with a brightness of 17.35 mag in the *Gaia*  $G$ -band. The discovery was reported on the *Gaia* Photometric Science Alerts Website on May 18. The last *Gaia* non-detection, with a limiting magnitude of  $\geq 20.5$  mag, is from April 5.2 UT. Later  $g$ -band non-detections on April  $9.7 \pm 8.5$  d (co-added) and April 18.3, down to limiting magnitudes of 22.1 mag and 21.0 mag respectively, were made by the Intermediate Palomar Transient Factory<sup>2</sup> (iPTF). The target was recovered in images taken with the Palomar 60-inch Telescope (P60) on May 12.3 (MJD 57520.32) at  $g = 17.3 \pm 0.2$  mag (Yan et al. 2016). The redshift of the event was determined to be  $z = 0.102$  using host galaxy lines, resulting in an absolute discovery magnitude of  $\sim -21.0$  mag. It was thus classified by Kangas et al. (2016) as a type I SLSN using the 2.56-m Nordic Optical Telescope (NOT; Djupvik & Andersen 2010) as part of the NOT Un-biased Transient Survey (NUTS; Mattila et al. 2016)<sup>3</sup>.

### 2.2 Host galaxy

Figure 1 shows the location of the SN and its faint host galaxy in our first  $r$ -band image from NOT/ALFOSC and a pre-explosion ESO Digitized Sky Survey image, with the field stars that have been used for calibrating the NOT images (see Section 2.3). The  $g$ -band magnitude of the host galaxy SDSS J120251.71+441527.4 is  $21.73 \pm 0.06$  mag according to SDSS Data Release 13. Thus the non- $K$ -corrected absolute magnitude is  $M_g = -16.69 \pm 0.07$  mag, consistent with the faint dwarf galaxies that typically host type I SLSNe (Leloudas et al. 2015; Lunnan et al. 2015; Perley et al. 2016). Narrow, persistent Balmer emission lines and [O III]  $\lambda\lambda 4959, 5007$  attributed to the host galaxy are visible in each spectrum of Gaia16apd (see Section 2.4). Using these narrow lines, we derived a redshift of  $z = 0.102 \pm 0.001$ , which was adopted for Gaia16apd. We estimated an upper limit for the [N II]  $\lambda 6584$  / H  $\alpha$  ratio as  $\log [\text{N II}]\lambda 6584 / \text{H } \alpha \lesssim -0.80$  dex. The measured average [O III]  $\lambda 5007$  / H  $\beta$  ratio is  $\log [\text{O III}]\lambda 5007 / \text{H } \beta = 0.68 \pm 0.05$  dex. These values are again consistent with other type I SLSN host galaxies. Thus the host galaxy of Gaia16apd seems typical for a type Ic SLSN. Using the  $R_{23}$  diagnostic (Kobulnicky et al. 1999), we obtain an estimated metallicity of  $0.2Z_\odot$ , in agreement with Nicholl et al. (2016a).

No Na I D absorption lines from the ISM in the host galaxy were detected in the optical spectra. However, the

<sup>1</sup> <http://gsaweb.ast.cam.ac.uk/alerts/>

<sup>2</sup> <http://www.ptf.caltech.edu/iptf>

<sup>3</sup> [csp2.lco.cl/not](http://csp2.lco.cl/not)

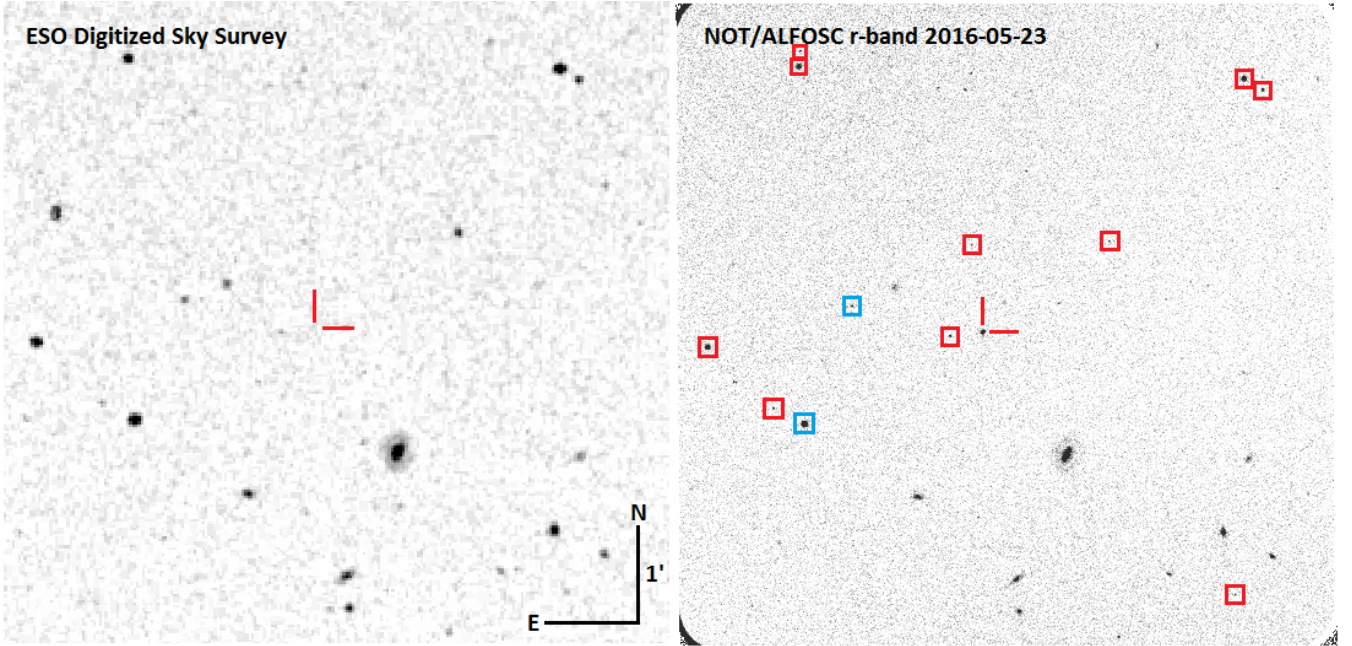


**Figure 1.** ESO Digitized Sky Survey image of the field of Gaia16apd (left) and our first  $r$ -band image from NOT/ALFOSC (right). The position of Gaia16apd is indicated with red tick marks in both images, and the stars used in the photometric calibration of the optical NOT images have been marked with red squares. The 2MASS stars used to calibrate both the optical and the NIR images are marked with blue squares.

*HST*/COS spectrum from MJD 57541.2 (7.9 d before  $g$ -band peak) published by Yan et al. (2016) was used to roughly estimate the host galaxy extinction as follows. In Figure 2, we show the *HST*/COS spectrum in the wavelength range 1010–1560 Å. Several spectral lines formed in the host galaxy of the SN and in the Milky Way are noted. In general, the host lines are somewhat stronger than lines formed in the Milky Way – particularly for the high-ionisation doublets C IV  $\lambda\lambda 1548, 1551$  and Si IV  $\lambda\lambda 1394, 1403$ , and to some extent Si III  $\lambda 1206$ . S II and Si II lines are more similar in strength for the two galaxies. We have overlaid modeled absorption profiles for L  $\alpha$  and L  $\beta$  for two column densities of neutral hydrogen in the host,  $N_{\text{H}}$ , namely  $1.5 \times 10^{20} \text{ cm}^{-2}$  (magenta) and  $2.5 \times 10^{20} \text{ cm}^{-2}$  (brown). Although the baselines for the absorption lines are not well defined, the fit for L  $\alpha$  suggests a column density between these numbers. Using the relation between  $E(B - V)$  and  $N_{\text{H}}$  of Gudennavar et al. (2012), this would result in  $E(B - V)_{\text{host}}$  in the 0.04 – 0.06 mag range assuming Solar metallicity. At the metallicity of the host,  $0.2Z_{\odot}$ , a range of 0.01 – 0.02 mag would be closer to the truth, considering the typical gas-to-dust mass as a function of metallicity (Rémy-Ruyer et al. 2014). Thus we adopt an estimated  $E(B - V)_{\text{host}} = 0.015 \pm 0.005$  mag, a slightly larger value than the foreground  $E(B - V)_{\text{gal}} = 0.0132$  mag, which is also indicated by the generally stronger host galaxy interstellar lines compared to the Milky Way ones. This results in a non-negligible correction in the UV, e.g.  $0.14 \pm 0.05$  mag in  $uvm2$ . A noticeable difference in strength is also noted for N I  $\lambda\lambda 1200, 1201$ , where the absorption in the host is much stronger than in the Milky Way, possibly indicating enhanced nitrogen abundance in the host.

### 2.3 Photometry

Optical and near-infrared (NIR) photometric follow-up observations were performed using the NOT. Optical imaging in the  $UBVri$  or  $uBVri$  bands was obtained using the Andalusia Faint Object Spectrograph and Camera (ALFOSC) instrument, while NIR imaging in the  $JHKs$  bands was obtained with the NOT near-infrared Camera and spectrograph (NOTCam) instrument. Optical photometric observations in the  $BVRI$  bands were also performed using the 0.5-m robotic telescope *pt5m* (Hardy et al. 2015) on La Palma, Canary Islands. UV and  $UBV$ -band photometry was performed with the Ultraviolet/Optical Telescope (UVOT) aboard *Swift* (the first *Swift* observations are reported in a telegram by Blagorodnova et al. 2016). We also included the public *Gaia* photometry points, converted to  $V$ -band according to Jordi et al. (2010), and the iPTF pre-discovery  $g$ -band point (Yan et al. 2016). Gaia16apd was observable until early August 2016, at which point it was obscured by the Sun. Observations resumed at the end of October 2016.

Reduction of the optical NOT images was done using the custom pipeline FOSCGUI<sup>4</sup>. The NIR data were reduced using a slightly modified version of the NOTCam Quicklook v2.5 reduction package<sup>5</sup>. Both use standard IRAF<sup>6</sup> tasks. The zero points of the  $uri$  images were calibrated relative to 12

<sup>4</sup> <http://sngroup.oapd.inaf.it/foscgui.html>

<sup>5</sup> <http://www.not.iac.es/instruments/notcam/guide/observe.html#reductions>

<sup>6</sup> IRAF is distributed by the National Optical Astronomy Observatory, which is operated by the Association of Universities for Research in Astronomy (AURA) under cooperative agreement with the National Science Foundation.



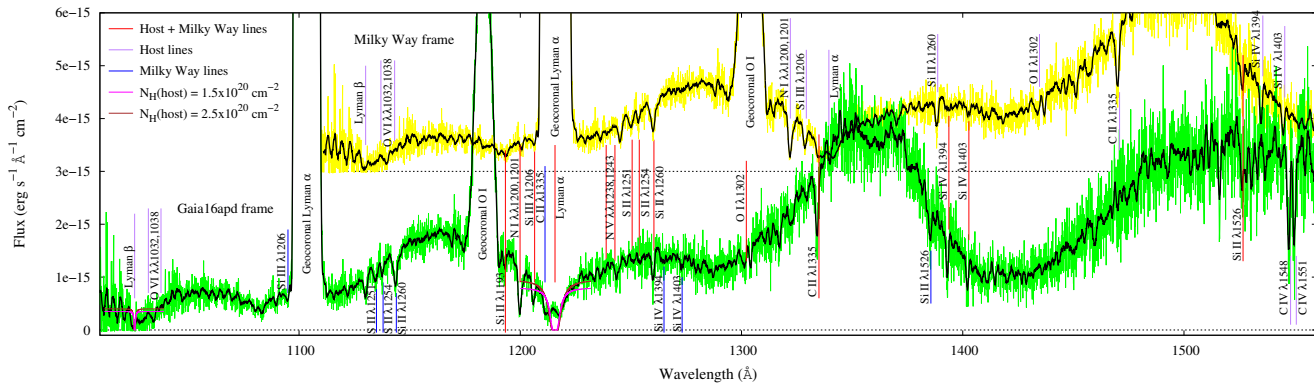


**Figure 2.** HST/COS spectrum of Gaia16apd at the rest frame of the SN (green) and in the Milky Way rest frame (i.e. the observed spectrum; yellow). The black spectra were obtained by Savitzky-Golay smoothing. The observed spectrum was shifted to facilitate comparisons. Spectral features indicated by red lines are formed both in the host galaxy of the SN and in the Milky Way. Blue lines indicate features originating in the Milky Way, and pink is for features originating in the host galaxy. In general, the line identifications are similar to those in [Yan et al. \(2016\)](#).

nearby stars with magnitudes available at the Sloan Digital Sky Survey (SDSS) Data Release 13 SkyServer<sup>7</sup>. The *UBV* magnitudes of the same field stars were calibrated using the standard star field GD 246 observed on the photometric night of 2016 July 13. The zero points of the *JHKs* images were calibrated relative to two nearby Two Micron All-Sky Survey (2MASS)<sup>8</sup> stars. The photometry was performed using the SNOOPy package<sup>9</sup> inside the QUBA pipeline (Valenti et al. 2011), which fits the point spread function (PSF) using the IRAF package DAOPHOT. Errors were estimated based on artificial star simulations around the SN position. Images from *pt5m* were reduced by an automatic pipeline that performs bias and flat-field correction and uses the SEXTRACTOR package to extract magnitudes. The *pt5m BVRi* images were photometrically calibrated by the Cambridge Photometric Calibration Server<sup>10</sup> using local SDSS stars and the conversion formulae by (Jordi et al. 2006). *Swift* photometry was reduced using the UVOTSOURCE task in the HEASOFT package.

The early photometry has not been corrected for host galaxy contamination. However, given that the host galaxy is faint,  $g = 21.73 \pm 0.06$  mag (over 4 mag fainter than the SN around peak), this contamination is on the order of a few per cent and has no significant effect on our analysis. At 130 d, the contamination is on the order of 15 per cent, and it has been subtracted from the late-time photometry. The photometry was corrected for Galactic extinction before  $K$ -correction, and for host extinction (see Section 2.2) after  $K$ -correction, using the Cardelli et al. (1989) law. SDSS magnitudes are reported in the AB system, while other magnitudes, including UV, are in the Vega system. A complete log of photometric observations is presented in Tables 1 (optical data), 2 (UV data) and 3 (NIR data). The *Swift* data before MJD 57591 have also been reported by Yan et al. (2016).

The optical photometry was  $K$ -corrected using the SuperNova Algorithm for  $K$ -correction Evaluation (SNAKE) code (Inserra et al. 2016) based on optical spectra of Gaia16apd.  $K$ -corrections in the  $U$  band were determined partially using blackbody fits to the spectra. *Swift* UV bands were  $K$ -corrected using *HST*/STIS spectra published by Yan et al. (2016). NIR bands were not  $K$ -corrected, as corrections using optical spectra were deemed unreliable. For intervening epochs,  $K$ -corrections were obtained by polynomial interpolation. The  $VRI$ -band data were  $K$ -corrected to the  $gri$  bands for clarity and to facilitate comparisons to other SLSNe.

The absolute magnitudes in all observed bands and the  $g - r$  colour evolution (after  $K$ - and extinction correction) are presented in Figure 3. We also show a comparison between Gaia16apd and three spectroscopically similar type Ic SLSNe, PTF12dam (Nicholl et al. 2013), SN 2010gx (Pastorello et al. 2010) and SN 2011ke (Inserra et al. 2013) in  $g$  and the *Swift* bands.

Using a low-order polynomial fit to the absolute  $g$ -band light curve, we obtained the peak epoch  $\text{MJD} = 57549.9 \pm 1.0$  d and peak magnitude  $M_{g,\text{peak}} = -21.8 \pm 0.1$  mag. The decline in the 30 rest-frame days after maximum is 0.9 mag. As shown in Figure 3, Gaia16apd declined faster at early times than the slowly-declining PTF12dam and similarly to SNe 2010gx and 2011ke, while being optically slightly brighter at peak. However, the late-time decline is slower than that of SN 2011ke, making Gaia16apd photometrically intermediate between the fast- and slowly-declining events.

Gaia16apd started off slightly bluer in  $g - r$  than SN 2010gx, evolving from roughly  $-0.6$  mag at  $-20$  d to  $\sim 0.3$  mag at 40 d. From  $\sim 10$  days after the maximum their colour evolution was similar. SN 2011ke remained  $\sim 0.4$  mag redder than Gaia16apd until 40 d, while PTF12dam started off redder but reddened more slowly. Gaia16apd reached an absolute magnitude of  $M_{uvm2} \simeq -23.6$  mag (Vega). However, as host extinction correction and  $K$ -correction in the UV have not been done in earlier SLSN studies, we here compare them to the non-corrected absolute magnitude of  $\sim -23.2$  mag. The *Swift*  $uvw1$  and  $uvw2$  filters suffer from

<sup>7</sup> <http://skyserver.sdss.org/dr13/en/home.aspx>

<sup>8</sup> <http://www.ipac.caltech.edu/2mass/>

<sup>9</sup> <http://sngroup.oapd.inaf.it/snoopy.html>

<sup>10</sup> <http://gsaweb.ast.cam.ac.uk/followup/>

**Table 1.** Log of optical photometric observations of Gaia16apd. SDSS magnitudes are reported in the AB system, while other magnitudes are in the Vega system. No  $K$ -corrections have been applied. The host galaxy magnitudes have been subtracted from points marked with an asterisk (\*).

Phase <sup>a</sup> (d)	MJD	Telescope	$u$ (mag)	$U$ (mag)	$B$ (mag)	$V$ (mag)	$r$ (mag)	$R$ (mag)	$i$ (mag)	$I$ (mag)
-22.8	57524.8	Gaia	—	—	—	17.39±0.06	—	—	—	—
-22.7	57524.9	Gaia	—	—	—	17.35±0.07	—	—	—	—
-18.3	57529.7	Swift	—	15.62±0.03	16.95±0.04	16.95±0.08	—	—	—	—
-16.5	57531.7	Swift	—	15.61±0.04	16.91±0.06	16.90±0.10	—	—	—	—
-16.2	57532.0	NOT	—	15.57±0.19	17.02±0.03	16.69±0.03	17.20±0.08	—	17.31±0.08	—
-15.4	57532.9	pt5m	—	—	—	—	—	17.07±0.03	—	—
-15.2	57533.2	Swift	—	15.43±0.05	16.69±0.07	16.75±0.12	—	—	—	—
-14.5	57533.9	pt5m	—	—	—	16.86±0.02	—	16.98±0.03	—	16.82±0.07
-13.6	57534.9	pt5m	—	—	—	—	—	16.96±0.02	—	—
-12.7	57535.9	NOT	16.43±0.19	—	16.82±0.03	16.48±0.03	17.01±0.04	—	17.13±0.04	—
-11.8	57536.9	pt5m	—	—	—	—	—	16.93±0.02	—	—
-11.3	57537.5	Swift	—	15.38±0.04	16.75±0.05	16.61±0.08	—	—	—	—
-10.0	57538.9	pt5m	—	—	—	—	—	16.81±0.04	—	—
-9.1	57539.9	pt5m	—	—	—	—	—	16.90±0.03	—	—
-8.2	57540.9	pt5m	—	—	—	—	—	16.83±0.02	—	16.67±0.05
-7.6	57541.5	Swift	—	15.26±0.04	16.60±0.05	16.52±0.08	—	—	—	—
-7.2	57542.0	NOT	—	15.32±0.18	16.70±0.04	16.41±0.04	16.81±0.04	—	16.90±0.04	—
-6.4	57542.9	pt5m	—	—	—	—	—	16.75±0.02	—	—
-6.0	57543.3	Swift	—	15.31±0.04	16.52±0.05	16.44±0.08	—	—	—	—
-5.4	57543.9	pt5m	—	—	—	—	—	16.76±0.02	—	16.59±0.05
-4.5	57544.9	pt5m	—	—	—	—	—	16.75±0.02	—	16.56±0.06
-4.2	57545.3	Swift	—	15.34±0.04	16.52±0.05	16.57±0.08	—	—	—	—
-3.6	57545.9	pt5m	—	—	—	16.56±0.03	—	16.69±0.02	—	—
-2.7	57546.9	pt5m	—	—	—	—	—	16.73±0.02	—	—
-2.4	57547.3	Swift	—	15.31±0.03	16.51±0.04	16.46±0.07	—	—	—	—
-1.8	57547.9	pt5m	—	—	—	—	—	16.69±0.02	—	16.53±0.06
0.6	57550.6	Swift	—	15.34±0.04	16.50±0.04	16.52±0.08	—	—	—	—
2.8	57553.0	NOT	—	15.37±0.17	16.70±0.04	16.30±0.04	16.77±0.08	—	16.85±0.08	—
3.1	57553.3	Swift	—	15.52±0.06	16.57±0.07	—	—	—	—	—
4.5	57554.9	Gaia	—	—	—	16.64±0.12	—	—	—	—
5.4	57555.9	pt5m	—	—	—	16.62±0.04	—	16.66±0.04	—	—
6.4	57556.9	Swift	—	15.52±0.04	16.59±0.05	16.51±0.08	—	—	—	—
8.6	57559.4	Swift	—	15.57±0.04	16.55±0.05	16.42±0.09	—	—	—	—
10.9	57561.9	pt5m	—	—	—	16.71±0.04	—	16.77±0.04	—	—
11.1	57562.1	Swift	—	15.78±0.05	16.73±0.05	16.61±0.08	—	—	—	—
12.7	57563.9	pt5m	—	—	—	16.65±0.06	—	—	—	—
12.8	57564.0	NOT	—	15.94±0.17	16.93±0.05	16.51±0.05	16.84±0.05	—	16.94±0.05	—
13.6	57564.9	pt5m	—	—	17.08±0.07	—	—	16.80±0.04	—	—
15.4	57566.9	pt5m	—	—	—	—	—	16.87±0.02	—	16.49±0.06
18.1	57569.9	pt5m	—	—	—	—	—	16.91±0.03	—	16.68±0.07
19.1	57571.0	NOT	—	16.36±0.24	17.38±0.03	16.73±0.03	17.06±0.05	—	16.94±0.05	—
21.0	57573.0	pt5m	—	—	—	17.18±0.03	—	—	—	—
21.8	57573.9	pt5m	—	—	—	—	—	17.05±0.02	—	16.67±0.05
22.7	57574.9	pt5m	—	—	—	—	—	16.96±0.02	—	16.71±0.08
28.9	57581.8	Gaia	—	—	—	17.40±0.08	—	—	—	—
29.0	57581.9	Gaia	—	—	—	17.37±0.06	—	—	—	—
37.2	57590.9	NOT	—	—	18.42±0.08	17.33±0.07	17.45±0.06	—	17.25±0.06	—
37.5	57591.2	Swift	—	17.77±0.18	18.52±0.24	17.71±0.25	—	—	—	—
40.9	57595.0	Swift	—	17.64±0.20	18.03±0.20	17.83±0.26	—	—	—	—
130.5	57693.7	NOT	—	—	—	*19.47±0.08	*19.68±0.10	—	*19.45±0.09	—
137.6	57701.5	Gaia	—	—	—	*19.82±0.08	—	—	—	—

<sup>a</sup> Rest-frame days since absolute  $g$ -band peak at MJD 57549.9.

**Table 2.** Log of *Swift* UV photometric observations of Gaia16apd. Magnitudes are reported in the Vega system. No  $K$ -corrections have been applied.

Phase (d)	MJD	$uvw2$ (mag)	$uvm2$ (mag)	$uvw1$ (mag)
-18.3	57529.7	15.71±0.04	15.27±0.04	15.15±0.04
-16.5	57531.7	15.76±0.04	15.26±0.04	15.19±0.05
-15.2	57533.2	15.77±0.04	—	15.14±0.05
-11.3	57537.5	15.82±0.04	15.37±0.04	15.16±0.04
-7.6	57541.5	15.91±0.04	15.40±0.04	15.16±0.04
-6.0	57543.3	15.97±0.05	15.53±0.05	15.24±0.05
-4.2	57545.3	16.15±0.04	15.66±0.04	15.36±0.05
-2.4	57547.3	16.11±0.05	15.67±0.04	15.41±0.04
0.6	57550.6	16.24±0.05	15.82±0.04	15.47±0.04
6.4	57556.9	16.63±0.05	16.22±0.05	15.95±0.05
8.6	57559.4	16.78±0.05	16.46±0.05	—
11.1	57562.1	17.18±0.05	16.62±0.05	16.25±0.06
37.5	57591.2	19.31±0.20	19.26±0.17	18.86±0.26
40.9	57595.0	19.08±0.26	19.40±0.31	18.50±0.28

**Table 3.** Log of NOT/NOTCam NIR photometric observations of Gaia16apd. Magnitudes are reported in the Vega system. No  $K$ -corrections have been applied.

Phase (d)	MJD	$J$ (mag)	$H$ (mag)	$K$ (mag)
1.0	57551.0	16.59±0.08	16.23±0.15	16.59±0.15
10.9	57561.9	16.32±0.08	16.79±0.15	16.85±0.15
30.9	57583.9	16.20±0.08	16.68±0.15	16.35±0.15
56.3	57611.9	17.13±0.08	17.36±0.15	17.25±0.15
140.9	57705.2	18.51±0.08	18.49±0.15	17.94±0.15

(which are not affected) of the comparison SNe are not  $K$ -corrected, we include  $uvw1$  here for the more distant comparison events where observed  $uvw1$  is close to  $uvm2$  as observed at  $z = 0.102$ . Gaia16apd was somewhat brighter in the UV than either PTF12dam or the fast-declining events of *Inserra et al. (2013)*. PTF11rks reached  $M_{uvm2} \simeq -20.8$  mag and  $M_{uvw1} \simeq -21.2$  mag – other SLSNe in the sample had no early *Swift* observations, but were between 0.3 and 1.3 mag fainter than Gaia16apd at 25 – 30 d. PTF12dam reached  $M_{uvm2} \simeq -22.4$  mag and SN 2015bn,

significant ‘red leak’, i.e. contamination by redder photons (*Brown et al. 2010*). However, as the  $uvm2$  magnitudes

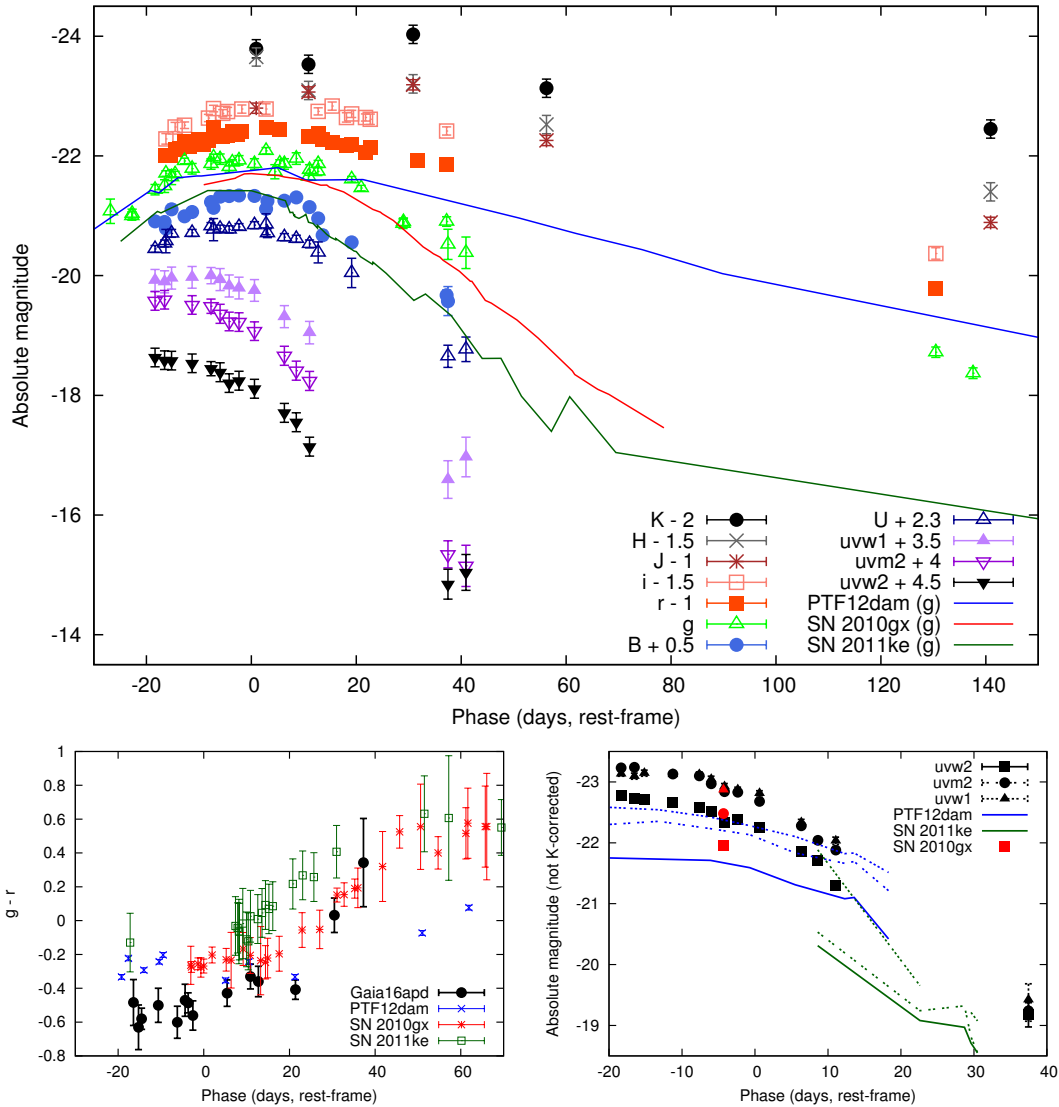


**Figure 3.** Extinction- and  $K$ -corrected absolute magnitude light curve (top),  $g-r$  colour evolution (bottom left) and UV light curve (bottom right) of Gaia16apd and three comparison events: PTF12dam (blue; Nicholl et al. 2013), SN 2010gx (red; Pastorello et al. 2010) and SN 2011ke (green; Inserra et al. 2013). The  $K$ -corrections of the comparison events (lines) were done using SNAKE and publicly available spectra. The reference date is the  $g$ -band peak.

another slowly-declining SLSN with good UV coverage, reached  $M_{uvw2} \simeq -22.5$  mag (Nicholl et al. 2016b). One early epoch of *Swift* data exists for SN 2010gx, yielding  $M_{uvw2} \simeq -22.5$  mag and  $M_{uvw1} \simeq -22.9$  mag at  $-5.6$  d, respectively 0.5 mag and 0.1 mag fainter than Gaia16apd at this epoch. At 10–15 d, the UV brightness had declined to the level of PTF12dam. In the NIR, both Gaia16apd and PTF12dam reached a non- $K$ -corrected  $M_H = -22.15$  mag (Vega) around  $g$ -band peak, but PTF12dam again declined slower afterwards.

## 2.4 Spectroscopy

Optical long-slit spectroscopic follow-up observations were performed using NOT/ALFOSC. The reduction of the spectroscopy was done using FOSGUI or the QUBA pipeline. Cosmic rays were removed using LACOSMIC (van Dokkum 2001).

Sensitivity curves were obtained using spectroscopic standard stars observed during the same night. A complete log of spectroscopic observations is presented in Table 4.

The spectra are presented in Figure 4, along with a comparison to PTF12dam, SN 2010gx and SN 2011ke. The spectra from  $-16.2$  d to 2.8 d are characterized by the distinctive O II absorption lines around 3500–4500 Å, typical for type Ic SLSNe (Quimby et al. 2011), with gradually decreasing velocity – the minimum of the  $\lambda\lambda 4415, 4417$  absorption changes from  $\sim -19800$  km s $^{-1}$  to  $\sim -15600$  km s $^{-1}$ . No other clear features were identified on top of the hot continua of the pre-peak spectra. By day 2.8, a weak Fe II  $\lambda 5169$  P Cygni profile is visible. By day 21.8, the O II lines had been replaced by Fe II absorption lines, Mg II  $\lambda 4481$  absorption and Mg I  $\lambda 4571$  emission, and the spectra resemble normal type Ic SNe around maximum light; this transition was still ongoing on day 12.8. O I  $\lambda 6156$  and  $\lambda 7774$  absorp-

**Table 4.** Log of spectroscopic observations of Gaia16apd. All spectra were obtained using NOT/ALFOSC, with grism #4 with a  $\lambda$  range of 3200 – 9600 Å and a dispersion of 3.3 Å pix<sup>−1</sup>, on the NOT.

Phase <sup>a</sup> (d)	MJD	Date	Slit width (arcsec)	Resolution (km/s)	Exposure (s)
−19.2	57528.9	2016 May 20.9	1.0	700	1800
−16.2	57532.0	2016 May 24.0	1.0	700	1800
2.8	57553.0	2016 June 14.0	1.3	900	1500
12.8	57564.0	2016 June 25.0	1.0	700	1500
21.8	57573.9	2016 July 4.9	1.0	700	1500
31.8	57584.9	2016 July 15.9	1.3	900	1500
43.6	57597.9	2016 July 28.9	1.0	700	1800
150.9	57716.2	2016 November 24.2	1.0	700	3600

<sup>a</sup> Rest-frame days since *g*-band peak at MJD 57549.9.

tion is also visible, along with a Ca II  $\lambda\lambda 3969, 3750$  P Cygni profile and Mg II  $\lambda\lambda 7877, 7896$  emission. The photospheric velocity, measured from the minima of the Fe II  $\lambda 5169$  absorption profiles, stayed nearly constant between days 2.8 and 43.6, evolving from  $\sim 12700$  km s<sup>−1</sup> to  $\sim 12400$  km s<sup>−1</sup>. Such a nearly flat velocity evolution is common among both fast- and slowly-declining type Ic SLSNe (Nicholl et al. 2015), as the central engine is expected to sweep most of the ejecta into a shell (Kasen & Bildsten 2010) instead of the normal homologous expansion scenario.

The features described above are common to type Ic SLSNe; as seen in the bottom panel of Figure 4, our comparison SNe show a somewhat similar evolution. The O II absorption lines in SN 2010gx disappeared somewhat faster, indicating a lower degree of ionization (temperature), as in the other events in Inserra et al. (2013), where O II was weak or nonexistent a few days after *g*-band peak. The slower-declining PTF12dam also only showed the O II lines until a few days before maximum light. The later evolution ( $\gtrsim 15$  d) was very similar in all these events. Figure 5 shows a clearer comparison between the late-time spectra of Gaia16apd (at 150.9 d) and the slowly declining SLSNe PTF12dam (at 171 d) and SN 2015bn (at 243 d). Gaia16apd displays a nebular spectrum at this phase, dominated by broad emission lines of calcium ([Ca II]  $\lambda\lambda 7291, 7324$  and the NIR triplet), oxygen ([O I]  $\lambda\lambda 6300, 6364$  and O I  $\lambda 7776$ ), sodium, magnesium and iron, at typical FWHM velocities of 10000 km s<sup>−1</sup>. An excess continuum blueward of  $\sim 5500$  Å is attributed to host galaxy contamination. The late spectra of Gaia16apd and PTF12dam are almost identical despite their different photometric evolution, with very similar emission line luminosities; the SN 2015bn spectrum is also strikingly similar despite the later epoch.

### 3 ANALYSIS

#### 3.1 SED and bolometric light curve

*K*- and extinction-corrected magnitudes were converted to fluxes to construct an SED for each epoch. Polynomial interpolation was used to obtain fluxes in all bandpasses for epochs where some filters were not used. A blackbody fit was used to approximate the wavelengths blueward of the *g* filter in the last point. Pseudo-bolometric luminosities were

calculated by integrating the SED over wavelength, assuming zero flux outside the used filters. Because of the significant ‘red leak’ suffered by the *Swift* *uvw1* and *uvw2* filters (Brown et al. 2010), the *uvm2* filter, which is not affected, was the only *Swift* filter used here. The *uvm2* and *U*-band fluxes were interpolated between 11 and 37 d using a quadratic fit to the light curve. A low-order polynomial fit to the pseudo-bolometric light curve yielded a peak epoch of MJD = 57539.2  $\pm$  0.5 d and a peak luminosity of  $2.8 \pm 0.1 \times 10^{44}$  erg s<sup>−1</sup>.

Blackbody functions were fitted to the fluxes using the MPFIT routine (Markwardt 2009) in IDL. We have also calculated blackbody temperatures using the pseudo-bolometric luminosity, assuming a constant expansion velocity of 12500  $\pm$  200 km s<sup>−1</sup>, a zero radius at explosion (since at this velocity, the radius of a star stripped of hydrogen is quickly reached) and an explosion epoch of MJD = 57514 (see Section 3.2). This gives an estimate of the intrinsic blackbody function before absorption in the UV and subsequent re-emission, which distorts the blackbody functions fitted to the optical SEDs, increasing optical fluxes at the expense of the UV fluxes. The evolution of the blackbody temperature, pseudo-bolometric luminosity and  $L_{griz}$  are presented in Figure 6. The temperature from the SED fit (pseudo-bolometric luminosity) evolved smoothly from  $\sim 23000$  K ( $\sim 20000$  K) at  $-18$  d to  $\sim 8000$  K ( $\sim 7000$  K) at 30 d. The estimated blackbody temperatures of other type I SLSNe are similar after the *g*-band peak, around 12000 – 14000 K at a few days, but somewhat cooler than Gaia16apd before it (Inserra et al. 2013; Nicholl et al. 2015, 2016a). This is consistent with how the *g* – *r* colour evolution of Gaia16apd compares to our comparison events.

For the purpose of comparison with the Nicholl et al. (2015) sample, we have also calculated  $L_{griz}$ , the luminosity over the *griz* filters. The *z*-band fluxes were estimated by integrating the SDSS *z*-band filter over the blackbody function at each epoch. These were then combined with the *gri* fluxes to construct an SED, which was integrated over wavelength assuming zero flux outside the *griz* filters, following Inserra et al. (2013). This *griz*-bolometric luminosity was expressed in the form of a magnitude, adapting the standard formula for the bolometric magnitude:

$$M_{griz} = -2.5 \log_{10} \frac{L_{griz}}{3.055 \times 10^{35} \text{ erg s}^{-1}}. \quad (1)$$

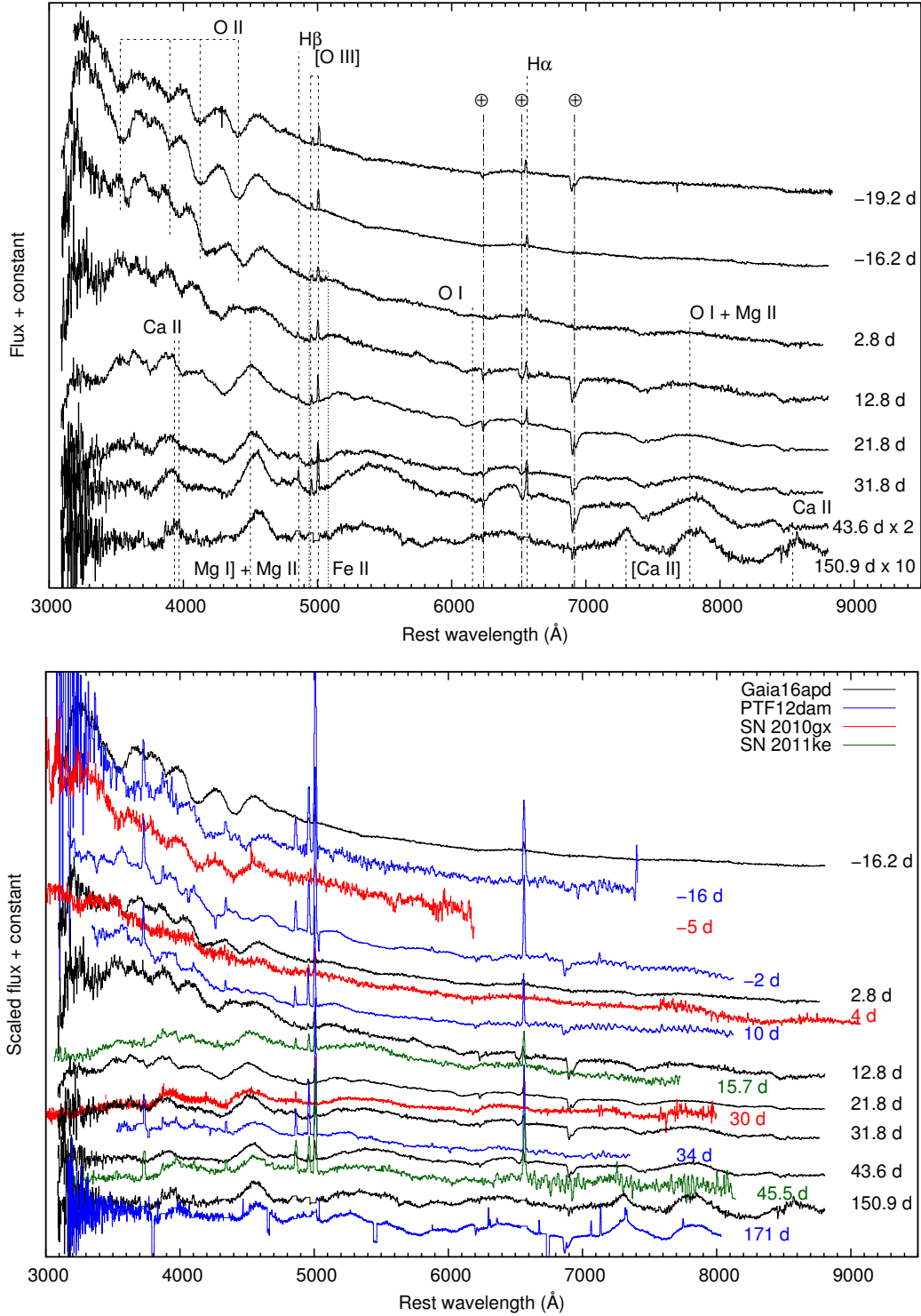


**Figure 4.** Spectral evolution of Gaia16apd (top) and a comparison to other type Ic SLSNe, SN 2010gx (Pastorello et al. 2010), PTF12dam (Nicholl et al. 2013) and SN 2011ke (Inserra et al. 2013) (bottom). The Gaia16apd spectra show prominent O II absorption lines at early stages, typical for type Ic SLSNe. Strong, narrow host galaxy lines have been removed from late-time ( $> 50$  d) spectra for clarity. The reference date is the  $g$ -band peak after  $K$ -correction for Gaia16apd and SN 2011ke, the  $r$ -band peak for PTF12dam and the  $B$ -band peak for SN 2010gx.



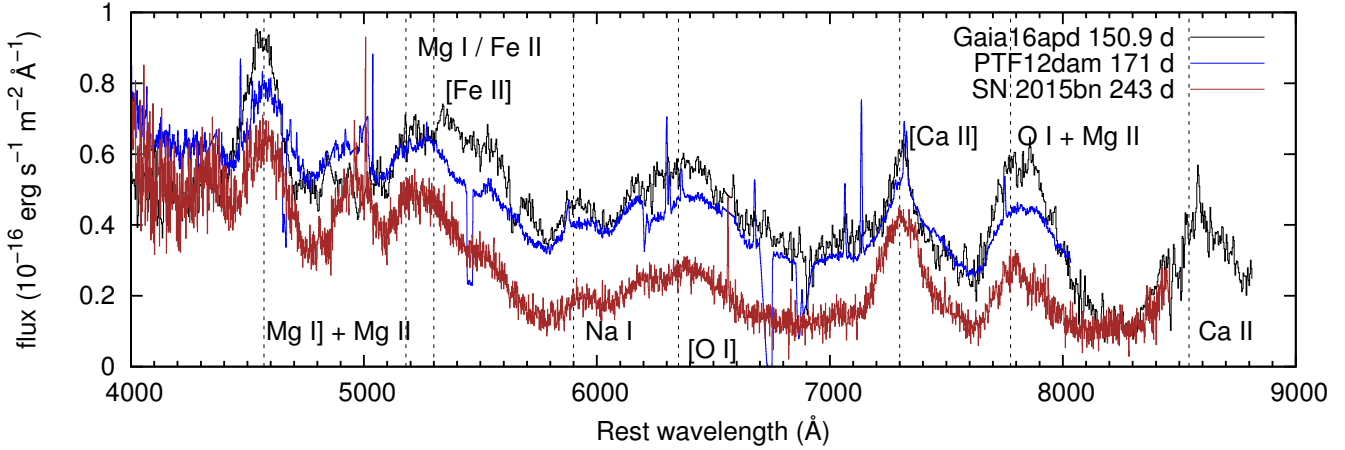


**Figure 5.** Comparison of late-time spectra of Gaia16apd (black), PTF12dam (blue; Nicholl et al. 2013) and SN 2015bn (brown; Nicholl et al. 2016b), demonstrating their similarity. Line identifications are based on Nicholl et al. (2013) and Jerkstrand et al. (2016). The spectra have been calibrated using photometry and corrected for extinction. Strong, narrow host galaxy lines have been removed for clarity.

Using a low-order polynomial fit, the *griz* luminosity peak was estimated as  $\text{MJD} = 57550.3 \pm 0.6$  d and the peak  $M_{griz}$  as  $-21.0 \pm 0.1$  mag, somewhat brighter than most fast-declining type Ic SLSNe but similar to SN 2005ap (Nicholl et al. 2015). From this fit, we also estimated the *e*-folding rise time  $\tau_{\text{rise}}$  of the *griz*-band luminosity as 27 d. The decline time  $\tau_{\text{dec}}$  was estimated as 47 d. Both values must be considered rough estimates, as these time-scales are not covered by our multi-band photometry. The  $\tau_{\text{dec}}$  is between the typical values for fast- and slowly-declining events. The values are, however, somewhat consistent with the empirical  $\tau_{\text{dec}} \approx 2\tau_{\text{rise}}$  relation; this supports a magnetar origin, as such a tight relation is difficult to explain using CSM interaction models (by e.g. Chatzopoulos et al. 2012) without fine-tuning the mass and density of the CSM (Nicholl et al. 2015).

### 3.2 Modelling

The injection of rotational energy from the rapid spin-down of a newborn highly magnetized neutron star (magnetar), with a magnetic field  $B$  in a range of  $10^{14} - 10^{15}$  G and an initial spin period  $P$  of a few ms, can significantly boost the optical luminosity of a SN (Kasen & Bildsten 2010; Woosley 2010). Millisecond magnetar models have been successfully employed to reproduce the light curves of type I SLSNe (e.g. Chomiuk et al. 2011; Inserra et al. 2013; Lunnan et al. 2016).  $P$  determines the rotational energy  $E_p \simeq 2 \times 10^{52} \text{ erg} \times (P/1 \text{ ms})^{-2}$ , while  $B$  and  $P$  together determine the spin-down time-scale  $\tau_p \simeq 4.7 \text{ d} \times (P/1 \text{ ms})^2 \times (B/10^{14} \text{ G})^{-2}$ . The third input parameter, the diffusion time in the ejecta  $\tau_m$ , is determined by the opacity  $\kappa$ , ejecta mass  $M_{\text{ej}}$  and kinetic energy  $E_k$  as

$$\tau_m = 10 \text{ d} \left( \frac{M_{\text{ej}}}{1 M_{\odot}} \right)^{3/4} \left( \frac{E_k}{10^{51} \text{ erg}} \right)^{-1/4} \left( \frac{\kappa}{0.1 \text{ cm}^2 \text{ g}^{-1}} \right)^{1/2}. \quad (2)$$

The luminosity evolution  $L(t)$  of the SLSN, assuming it to be dominated by the magnetar power, is then described by

$$L(t) = \frac{2E_p}{\tau_p \tau_m} e^{-(t/\tau_m)^2} \int_0^t \frac{1}{(1+t'/\tau_p)^2} e^{(t'/\tau_m)^2} \frac{t' dt'}{\tau_m}. \quad (3)$$

This model was fitted to the pseudo-bolometric light curve of Gaia16apd using Markov Chain Monte Carlo (MCMC) simulations based on the PYTHON package EMCEE (Foreman-Mackey et al. 2013). We used 40,000 iterations in total, while discarding the initial 10,000 as part of the burn-in sample. The best values were derived using the maximum of the posterior probability distribution, and the error bars correspond to  $1 \sigma$  integrated probability towards lower and upper values of the distribution. The best-fitting input parameters were  $P = 1.9^{+0.3}_{-0.2}$  ms,  $B = 2.1^{+0.5}_{-0.2} \times 10^{14}$  G and  $\tau_m = 37^{+2}_{-3}$  d. The derived explosion date was  $\text{MJD} = 57514$  (from a rise time of 25 d), and the total radiated energy from the model was  $1.4 \times 10^{51}$  erg over 1000 d. The best-fitting magnetar light curve is shown in Figure 6. At 135 d, there is a difference of  $\sim 0.2$  dex between the model and the pseudo-bolometric light curve, but as the model is fairly simple, a perfect match at late times may be unrealistic. Using Eq. (5) of Nicholl et al. (2015), we estimated the ejecta mass as

$$M_{\text{ej}} = 7.7 \times 10^{-7} M_{\odot} \times \left( \frac{\kappa}{0.1 \text{ cm}^2 \text{ g}^{-1}} \right)^{-1} \frac{v}{\text{km s}^{-1}} \left( \frac{\tau_m}{\text{d}} \right)^2, \quad (4)$$

where  $v$  is approximately the photospheric velocity, measured using the minima of Fe II  $\lambda 5169$  absorption lines. As the velocity evolution of this line was nearly flat, we use the same value as for the blackbody calculation, 12500 km s<sup>-1</sup>. Assuming  $\kappa = 0.1 \text{ cm}^2 \text{ g}^{-1}$  (typical in normal type Ic SNe), the resulting estimated ejecta mass is  $\sim 13 M_{\odot}$  (with  $E_k \simeq 2.1 \times 10^{52}$  erg), while with  $\kappa = 0.2 \text{ cm}^2 \text{ g}^{-1}$  (full ionization), the result is  $\sim 7 M_{\odot}$  ( $E_k \simeq 1.0 \times 10^{52}$  erg) – the latter estimate is close to the ejecta masses of some abnormal type Ic SNe (Valenti et al. 2012; Taddia et al. 2016). A high degree of ionization could be caused by hard radiation from the magnetar (Metzger et al. 2014).

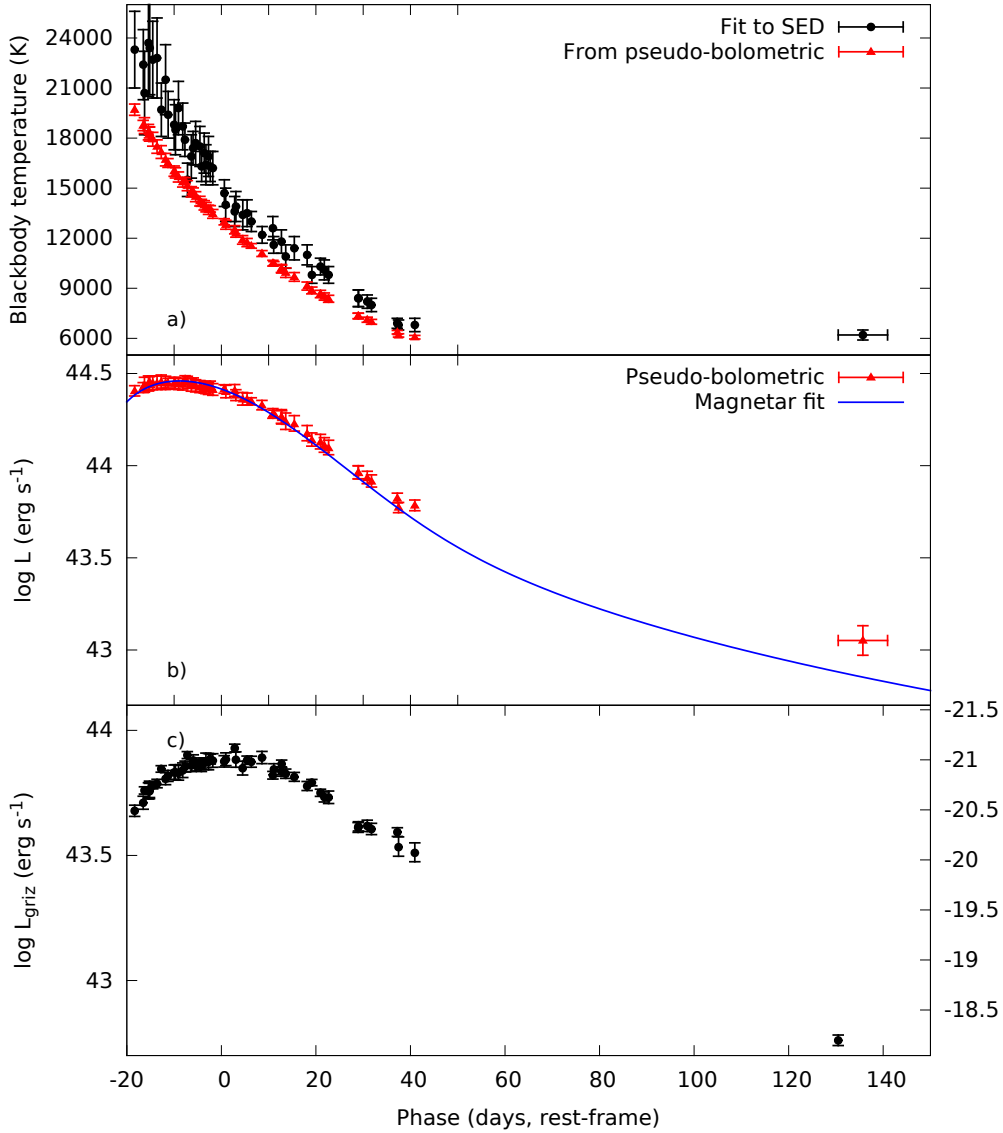


**Figure 6.** Evolution of the blackbody temperature (a), pseudo-bolometric luminosity (b) and *griz*-band luminosity (c) of Gaia16apd. The red dots in (a) have been calculated based on the pseudo-bolometric luminosity and a constant expansion speed of  $12500 \text{ km s}^{-1}$ . The blue line in (b) is a magnetar model fit with magnetic field  $2.1 \times 10^{14} \text{ G}$ , period  $1.9 \text{ ms}$  and diffusion time  $37 \text{ d}$ .

The kinetic energy has been estimated assuming that the entire mass of the ejecta is swept up into a thin shell and moves at the same velocity, which is a reasonable approximation in the magnetar scenario (Kasen & Bildsten 2010). Nicholl et al. (2016a) arrive at a much lower value of  $2.4 \times 10^{51} \text{ erg}$  despite very similar magnetar parameters – which they acknowledge as a probable underestimate, as they assume homologous expansion. The true value is likely somewhere between these estimates. The ejecta mass and kinetic energy estimated by Yan et al. (2016) are closer to ours.

#### 4 DISCUSSION AND CONCLUSIONS

We have presented observations of Gaia16apd, one of the closest SLSNe ever discovered ( $z = 0.102$ ), in a wavelength range spanning the *Swift* UV bands, the optical region and NIR. Spectroscopically Gaia16apd is a typical type Ic SLSN; photometrically, it is intermediate between fast-declining type Ic SLSNe such as SN 2011ke and slowly-declining ones such as PTF12dam. While its peak absolute magnitudes of  $M_g = -21.8 \pm 0.1$  and  $M_{griz} = -21.0 \pm 0.1$  are at the bright end of the fast-declining class, with a *g*-band decline of 0.9 mag in the first 30 d after peak it is consistent with the Inserra & Smartt (2014) peak-decline relation for SN 2005ap-like events. The host galaxy is a faint, low-metallicity dwarf

galaxy consistent with those of other type Ic SLSNe (Perley et al. 2016).

The nearly constant Fe II  $\lambda 5169$  line velocity is consistent with a swept-up shell in a magnetar-powered explosion (Kasen & Bildsten 2010). Furthermore, Yan et al. (2016) found a lack of line blanketing in the UV spectra of Gaia16apd compared to normal SNe, caused by a lack of iron-group elements such as  $^{56}\text{Ni}$  in the ejecta, and concluded that a PISN scenario was implausible based on the low  $^{56}\text{Ni}$  mass (although, as shown by Nicholl et al. 2016a, the line blanketing is not significantly weaker than in other SLSNe). Nicholl et al. (2016a) excluded CSM interaction as a source of the UV brightness. We have thus fitted a grid of magnetar models to the pseudo-bolometric light curve and obtained best-fit parameters of  $P = 1.9^{+0.3}_{-0.2}$  ms,  $B = 2.1^{+0.5}_{-0.2} \times 10^{14}$  G and  $\tau_m = 37^{+2}_{-3}$  d. These values are consistent with those expected from newborn magnetars. The rise time to the bolometric peak was estimated as 25 d. The ejecta mass obtained using  $\tau_m$  and the Fe II  $\lambda 5169$  velocity is 6 or 13  $M_\odot$ , with opacities  $\kappa = 0.2$  (possible for magnetar-powered explosions; Metzger et al. 2014) or  $0.1 \text{ cm}^2 \text{ g}^{-1}$ , respectively. The ejecta mass and decline time-scale are between the typical values for fast- and slowly-declining type Ic SLSNe, but Gaia16apd does conform to the  $\tau_{\text{dec}} \approx 2\tau_{\text{rise}}$  relation that the magnetar scenario produces (Nicholl et al. 2015). Some unusual type Ic SNe have had similar ejecta masses (such as SN 2011bm; Valenti et al. 2012); such an event combined with the magnetar spin-down energy input is consistent with Gaia16apd.

Gaia16apd exhibited UV magnitudes significantly brighter than those of slow-declining type Ic SLSNe with UV coverage. Of the fast-declining events, only SN 2010gx showed a similar early UV brightness. The pre-peak temperature of Gaia16apd was somewhat higher than usual for its class, consistently with the early colour evolution and UV brightness. Yan et al. (2016) argued that the lack of iron-group elements in the outer ejecta is the main reason for the UV brightness, while Nicholl et al. (2016a) showed that it can simply be explained with the right combination of magnetar parameters. With our magnetar fit, the central engine power (which determines the colour of the spectrum as shown in Figure 11 of Howell et al. 2013) is consistent with theirs, and we agree with the latter interpretation. This event highlights the importance of good rest-frame UV coverage. Apart from SN 2010gx, other similarly UV-bright examples are not known so far, possibly because of insufficient UV observations. SLSNe have been proposed as standard candles observable at high redshift (Inserra & Smartt 2014; Scovacricchi et al. 2016), which will require a robust description and understanding of their UV variability.

The late-time spectrum at 150.9 d is very similar to that of PTF12dam at 171 d, with slightly higher line luminosities. Jerkstrand et al. (2016) applied nebular-phase models to the late-time spectra of slowly-declining type Ic SLSNe and showed them to be consistent with  $\gtrsim 10M_\odot$  of oxygen-rich ejecta, which places a limit of  $\gtrsim 40M_\odot$  on the Wolf-Rayet progenitor in a single-star scenario. The striking similarity between Gaia16apd and PTF12dam, and by proxy other slowly-declining type Ic SLSNe, suggests that this may also hold true for at least some fast-declining events. For Gaia16apd, it is also consistent with our estimate of the ejecta mass from the magnetar model. PISN and CSM in-

teraction models do not seem to match observations of either class (e.g. Nicholl et al. 2014; McCrum et al. 2014; Yan et al. 2016; Lunnan et al. 2016), and a millisecond magnetar scenario is now widely considered to be the most likely one for both. Another implication is that the two classes may form a continuum of properties instead of having discrete progenitor populations.

## ACKNOWLEDGEMENTS

We thank Subo Dong, Cosimo Inserra, Christa Gall and Andrea Pastorello for their suggestions.

We acknowledge ESA Gaia, DPAC and the Photometric Science Alerts Team (<http://gsaweb.ast.cam.ac.uk/alerts>). The *pt5m* photometric calibrations were obtained using the Cambridge Photometric Calibration Server (CPCS), designed and maintained by Sergey Koposov and Lukasz Wyrzykowski.

Based on observations made with the Nordic Optical Telescope, operated by the Nordic Optical Telescope Scientific Association at the Observatorio del Roque de los Muchachos, La Palma, Spain, of the Instituto de Astrofísica de Canarias. The data presented here were obtained in part with ALFOSC, which is provided by the Instituto de Astrofísica de Andalucía (IAA) under a joint agreement with the University of Copenhagen and NOTSA.

J. H. acknowledges support by the Finnish Cultural Foundation. M. F. acknowledges the support of a Royal Society - Science Foundation Ireland University Research Fellowship. N. E. R. acknowledges financial support by the 1994 PRIN-INAF 2014 (project ‘Transient Universe: unveiling new types of stellar explosions with PESSTO’) and by MIUR PRIN 2010- 2011, ‘The dark Universe and the cosmic evolution of baryons: from current surveys to Euclid’. E. Y. H. acknowledges the support provided by the National Science Foundation under Grant No. AST-1008343 and AST-1613472. M. D. S. is funded by generous support provided by the Danish Agency for Science and Technology and Innovation realised through a Sapere Aude Level 2 grant, and a grant from the Villum Foundation. NUTS is funded in part by the IDA (Instrument Centre for Danish Astronomy). L. W. was supported by Polish National Science Centre grant OPUS 2015/17/B/ST9/03167.

## REFERENCES

- Bennett C. L., Larson D., Weiland J. L., Hinshaw G., 2014, *ApJ*, **794**, 135
- Blagorodnova N., Yan L., Quimby R., Olaes M. K., Brown P., Cooke J., 2016, *The Astronomer’s Telegram*, **9074**
- Brown P. J., et al., 2010, *ApJ*, **721**, 1608
- Cardelli J. A., Clayton G. C., Mathis J. S., 1989, *ApJ*, **345**, 245
- Chatzopoulos E., Wheeler J. C., Vinko J., 2012, *ApJ*, **746**, 121
- Chen T.-W., et al., 2013, *ApJ*, **763**, L28
- Chen T.-W., et al., 2015, *MNRAS*, **452**, 1567
- Chevalier R. A., Irwin C. M., 2011, *ApJ*, **729**, L6
- Chomiuk L., et al., 2011, *ApJ*, **743**, 114
- Dessart L., Waldman R., Livne E., Hillier D. J., Blondin S., 2013, *MNRAS*, **428**, 3227
- Dexter J., Kasen D., 2013, *ApJ*, **772**, 30
- Djupvik A. A., Andersen J., 2010, *Astrophysics and Space Science Proceedings*, **14**, 211

- Foreman-Mackey D., Hogg D. W., Lang D., Goodman J., 2013, *PASP*, **125**, 306
- Gaia Collaboration 2016, preprint, ([arXiv:1609.04153](#))
- Gal-Yam A., 2012, *Science*, **337**, 927
- Gal-Yam A., et al., 2009, *Nature*, **462**, 624
- Gudennavar S. B., Bubbly S. G., Preethi K., Murthy J., 2012, *ApJS*, **199**, 8
- Hardy L. K., Butterley T., Dhillon V. S., Littlefair S. P., Wilson R. W., 2015, *MNRAS*, **454**, 4316
- Heger A., Woosley S. E., 2002, *ApJ*, **567**, 532
- Howell D. A., et al., 2013, *ApJ*, **779**, 98
- Inserra C., Smartt S. J., 2014, *ApJ*, **796**, 87
- Inserra C., et al., 2013, *ApJ*, **770**, 128
- Inserra C., et al., 2016, preprint, ([arXiv:1604.01226](#))
- Jerkstrand A., et al., 2016, preprint, ([arXiv:1608.02994](#))
- Jordi K., Grebel E. K., Ammon K., 2006, *A&A*, **460**, 339
- Jordi C., et al., 2010, *A&A*, **523**, A48
- Kangas T., et al., 2016, The Astronomer’s Telegram, **9071**
- Kasen D., Bildsten L., 2010, *ApJ*, **717**, 245
- Kasen D., Woosley S. E., Heger A., 2011, *ApJ*, **734**, 102
- Kobulnicky H. A., Kennicutt Jr. R. C., Pizagno J. L., 1999, *ApJ*, **514**, 544
- Leloudas G., et al., 2015, *MNRAS*, **449**, 917
- Lunnan R., et al., 2015, *ApJ*, **804**, 90
- Lunnan R., et al., 2016, *ApJ*, **831**, 144
- Markwardt C. B., 2009, in Bohlender D. A., Durand D., Dowler P., eds, *Astronomical Society of the Pacific Conference Series* Vol. 411, *Astronomical Data Analysis Software and Systems XVIII*. p. 251 ([arXiv:0902.2850](#))
- Mattila S., et al., 2016, The Astronomer’s Telegram, **8992**
- McCrum M., et al., 2014, *MNRAS*, **437**, 656
- McCrum M., et al., 2015, *MNRAS*, **448**, 1206
- Metzger B. D., Vurm I., Hascoët R., Beloborodov A. M., 2014, *MNRAS*, **437**, 703
- Nicholl M., et al., 2013, *Nature*, **502**, 346
- Nicholl M., et al., 2014, *MNRAS*, **444**, 2096
- Nicholl M., et al., 2015, *MNRAS*, **452**, 3869
- Nicholl M., Berger E., Margutti R., Blanchard P. K., Milisavljevic D., Challis P., Metzger B. D., Chornock R., 2016a, preprint, ([arXiv:1611.06993](#))
- Nicholl M., et al., 2016b, *ApJ*, **826**, 39
- Pastorello A., et al., 2010, *ApJ*, **724**, L16
- Perley D. A., et al., 2016, *ApJ*, **830**, 13
- Quimby R. M., et al., 2011, *Nature*, **474**, 487
- Quimby R. M., Yuan F., Akerlof C., Wheeler J. C., 2013, *MNRAS*, **431**, 912
- Rémy-Ruyer A., et al., 2014, *A&A*, **563**, A31
- Schlaflly E. F., Finkbeiner D. P., 2011, *ApJ*, **737**, 103
- Scovaccicchi D., Nichol R. C., Bacon D., Sullivan M., Prajs S., 2016, *MNRAS*, **456**, 1700
- Taddia F., et al., 2016, *A&A*, **592**, A89
- Valenti S., et al., 2011, *MNRAS*, **416**, 3138
- Valenti S., et al., 2012, *ApJ*, **749**, L28
- Woosley S. E., 2010, *ApJ*, **719**, L204
- Yan L., et al., 2016, preprint, ([arXiv:1611.02782](#))
- van Dokkum P. G., 2001, *PASP*, **113**, 1420

This paper has been typeset from a  $\text{\TeX}/\text{\LaTeX}$  file prepared by the author.